# Determination of the Descriptors for the Design of a Classifier that Allows the Detection of Loss of Material in Metal Sheets Based on Signals of non-Destructive Tests

Hernando González, Carlos Arizmendi, Javier Quintero
Universidad Autónoma de Bucaramanga - UNAB
Bucaramanga, Colombia
e-mail: hgonzalez7@unab.edu.co,
carizmendi@unab.edu.co, jquintero20@unab.edu.co

Mario A. Quintero
Corporation for corrosion research
Universidad Industrial de Santander
Bucaramanga, Colombia
e-mail: mquintero@corrosion.uis.edu.co

***Abstract*—The article proposes a methodology to determine appropriate descriptors for the design of a classifier based on neural networks that allow the detection of loss of material in metal pipes based on nondestructive testing signals of Magnetic Flux Leakage (MFL). For this it has been proposed a method which consists of two stages: the first, corresponding to the signal processing, the Discrete Wavelet Transform (DWT) transform is used to implement a nonlinear threshold filtering or Shrinkage and correction baseline which seeks to eliminate or mitigate the different types of noise or phenomena found in the signal that make difficult the process of extracting relevant information to the subsequent detection of loss of material. In the second, corresponding to the design of the classifier, it seeks to identify a window width and descriptors in the time domain and the Power Spectral Density (PSD) to characterize the signal and differentiate areas of metal loss or no metal loss.**

***Keywords-magnetic flux leakage; discrete wavelet transform; power spectral density; artificial neural networks***

## I. INTRODUCTION

In hydrocarbon transport lines of great lengths it is not possible to carry out a manual inspection of loss of adequate preventive material because the geographical conditions are not favorable for the workers and often the fault is difficult to access, making it difficult to detect them. The inspection tools usually require a present operator who analyzes the collected information and identifies defects, so the results will depend on a human factor, increasing the degree of uncertainty.

The Integrity and Operation Trends Inspection (ITION) project of the Corporation for Corrosion Research (CIC) seeks to develop a pipe inspection device for the transport of hydrocarbons in order to detect references, obstructions and critical defects in the wall of the pipe. For the detection of critical defects, the device applies a technique called Magnetic Flux Leakage (MFL), which consists of generating a magnetic field that temporarily magnetizes the duct and by means of sensors recording field leaks that may occur, these signals are directly related to the current state of the pipe. The technique has been used in [1], [2], [3], [4] and [5], using different methods that allow a better interpretation of the signal, implementing adaptive filters to remove noise, wavelet transform to characterize the loss of material, neural networks to determine a model, among others.

## II. MFL SIGNALS

Non-destructive testing techniques range from ultrasound, radiography and electromagnetism among others. The first inspection methods involved high-frequency ultrasonic signals to detect external cracks and defects in the pipes. These first inspection techniques represented a difficult problem of modeling and complex signal interpretation algorithms, besides the ultrasonic inspection only allowed to detect surface problems and it was impossible to identify the internal state of the pipe without making a precise scan on the surface of the material.

Electromagnetic inspection is an alternative technique proposed for the ultrasonic inspection of pipes in the 70s [6]. This new form of inspection consisted of applying a magnetic field to the duct and measuring the magnetic field leakage to detect the presence of defects. The reason for this leak is the reduction in the cross-sectional area of the pipe wall so it cannot allow the passage of more magnetic flux, consequently the only way that the magnetic field lines can follow is to jump to an area of where the cross-sectional area increases again and enters the pipeline. Because the magnetic flux is a vector quantity, it can be measured in each of its components: axial, radial and transverse. The MFL technique, together with the X-ray and Eddy currents, became highly used techniques for the detection of internal faults in the wall of the pipeline [7].

Figure 1 illustrates the operating principle of MFL where a change in the behavior of the magnetic flux (1) can be seen once they encounter a defect (2). The permanent magnets (3) are responsible for producing the magnetic flux, the brushes (4) ensure contact between the permanent magnets and the wall of the pipe (5) in case of diameter variations and the yoke (6) closes the circuit magnetic.

For the development of the article, 8 radial MFL signals and one odometer signal were used, which are part of a database provided by the CIC, where each signal has 10'139.190 points sampled at 300Hz; the signals correspond to a run of approximately 23Km of the ITION device through a real pipeline. The database includes 3 marks of

978-1-5386-6987-7/18/$31.00 ©2018 IEEE

loss of significant material in the pipeline which are located at 600.72m, 8676.37m and 11291.64m. The data is labeled as follows: with <-1> the wave profile closest to a magnetic field leak is identified due to the presence of a defect in the pipe and with <+1> the section of the remaining pipe.

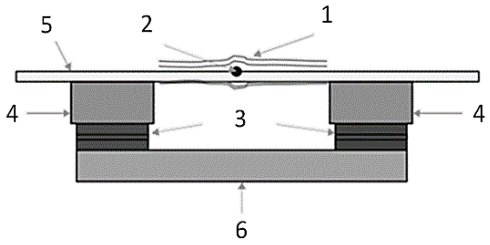


Figure 1. MFL operation diagram.

### A. Processing of MFL Signals

MFL signals can be strongly affected by noise levels from inherent pipeline artifacts, welds joining different sections, parasitic noise, thermal noise and from any electromagnetic source that may be operating in the area. To overcome this problem, we used a threshold filtering technique or Shrinkage [8] [9], the objective of this technique is to eliminate any noise that may be present in the signal, preserving the maximum information relevant to it, using the transformed wavelet.

TABLE I. MOTHER WAVELET AND MAXIMUM DECOMPOSITION LEVEL FOR EACH MFL SIGNAL

| Signal | Proper Mother Wavelet | Decomposition level |
|---|---|---|
| Signal 1 - MFL | Symlet 9 | 5 |
| Signal 2 - MFL | Symlet 9 | 5 |
| Signal 3 - MFL | Symlet 9 | 5 |
| Signal 4 - MFL | Symlet 9 | 5 |
| Signal 5 - MFL | Symlet 9 | 5 |
| Signal 6 - MFL | Symlet 9 | 5 |
| Signal 7 - MFL | Symlet 9 | 5 |
| Signal 8 - MFL | Symlet 9 | 5 |

The discrete wavelet transforms (DWT) breaks down the signal into high frequency components, also known as details, and low frequency components, called approximations. The Shrinkage filter applies the DWT to perform a multilevel decomposition, determining a threshold (λ) and a scaling factor (σ) based on the noise levels present in the signal. To apply this technique, it is necessary to identify the appropriate mother Wavelet for each signal, for this the criterion of the least mean square error (MSE) was used, equation 1, where x is the original signal, $\hat{x}$ is the reconstructed signal and N number of Signs of the signal. To determine the maximum level of decomposition, the Shannon entropy criterion was used, which measures the level of uncertainty or disorder of a system. Table 1 shows the mother wavelet function used for each of the eight MFL signals and the maximum decomposition level, obtaining the same function for each signal.

$$MSE = \frac{1}{N}\sum_{i=1}^{N}[x(i) - \hat{x}(i)] \quad (1)$$

Once the mother Wavelet and the appropriate decomposition level have been determined for each signal, we proceed to identify the threshold and scaling factor that allow filtering the signal without eliminating important information from it. To calculate the threshold, four methods were compared: universal threshold, Stein's impartial risk principle application threshold, minimax threshold and combination threshold, which are found in the Matlab® 2014 Wavelet toolbox under the names "Sqtwolog", "Rigrsure", "minimax", and "heursure" respectively. To determine threshold scaling, 3 methods were compared: unit scaling, Sln scaling and Mln scaling. Two methods were compared to implement the filter: Soft implementation and Hard implementation. To identify the appropriate methodology, the 8 signals were filtered with all possible combinations of the previously described methods and the minimum MSE between the original signal and the filtered signal was searched, the results are presented in table 2. Once the Shrinkage filter has been selected the best window width is determined to perform the filtering of the signals, for this the criterion of looking for the highest signal-to-noise ratio (SNR), between the filtered complete signal and the filtered signal with a determined window width, is applied. Equation 2 corresponds to the expression of the SNR, where x is the original signal, $\hat{x}$ is the reconstructed signal and N number of samples of the signal.

$$SNR(db) = 10\,log\left[\frac{\sum_{i=1}^{N}[x(i)]^2}{\sum_{i=1}^{N}[x(i)-\hat{x}(i)]}\right] \quad (2)$$

TABLE II. FILTRO SHRINKAGE PARA LAS SEÑALES MFL

| Signal | Threshold calculation | Threshold scaling | Implementation |
|---|---|---|---|
| Signal 1 - MFL | minimax | Unitary | Soft |
| Signal 2 - MFL | minimax | Unitary | Soft |
| Signal 3 - MFL | minimax | Unitary | Soft |
| Signal 4 - MFL | minimax | Unitary | Soft |
| Signal 5 - MFL | minimax | Sln | Soft |
| Signal 6 - MFL | minimax | Sln | Soft |
| Signal 7 - MFL | minimax | Sln | Soft |
| Signal 8 - MFL | minimax | Sln | Soft |

A sweep was made from 1,000 samples to 2,000,000 samples with 1,000 samples, the displacement of the rectangular window was made based on the size of the window used minus one sample; the overlapping sample between windows is equal to the average of the overlapping samples, if the last window is smaller than the window size used, the total number of missing samples is taken as the final window. The SNR for one of the eight signals are observed in Figure 2; the result was very similar for all signals in both variation and amplitude.

Since the variation of the SNR is minimal among all the window widths, a window width of 1'048,576 (210) samples

is selected since the algorithms used work efficiently when using window widths that are power of 2. In the figure 3 can see the results of the filtering on a section of one of the signals where a defect is found which is highlighted in a gray color, the result was similar for all the other eight signals.

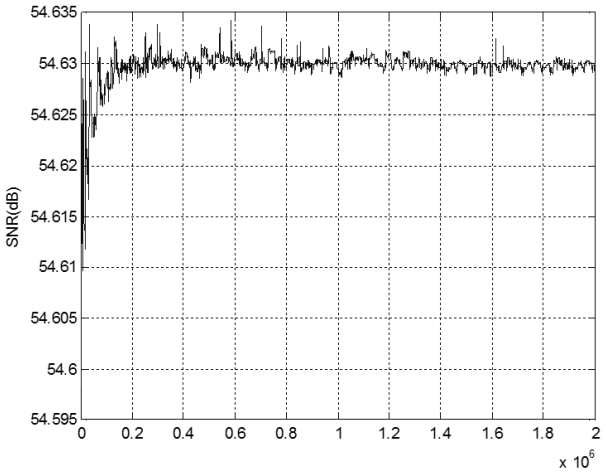


Figure 2. Signal to Noise Ratio (SNR) vs. window width.

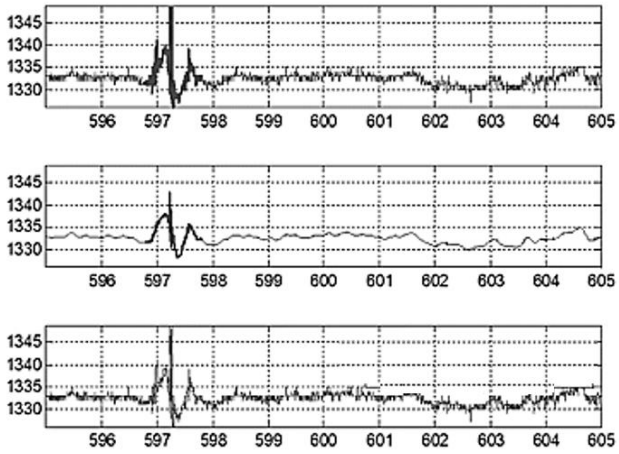

Figure 3. Shrinkage filter results on the first defect in the pipe. a) Original signal, b) Processed signal c) Original signal vs processed signal.

### *B. Base Line Correction*

In the eight MFL signals there is an offset or continuous level which can be the cause of some kind of hysteresis, remanence or natural dynamics of the system. This can be unfavorable or not at the time of discriminating between defect zones and no defect in the pipeline, which is why a multilevel decomposition is used to eliminate said component. It is proposed to work with two types of approaches, some called Aps1 which are those processed by the filtering Shrinkage and other calls Aps2 which are the same as the previous ones without the DC component [10]. To determine the level of offset, the components of the DWT approximations were analyzed, that is, decompose the signal at a level of detail and approximation, the following decompositions are made on the approximation levels, thus achieving to determine the most important components of low frequencies present in the signal.

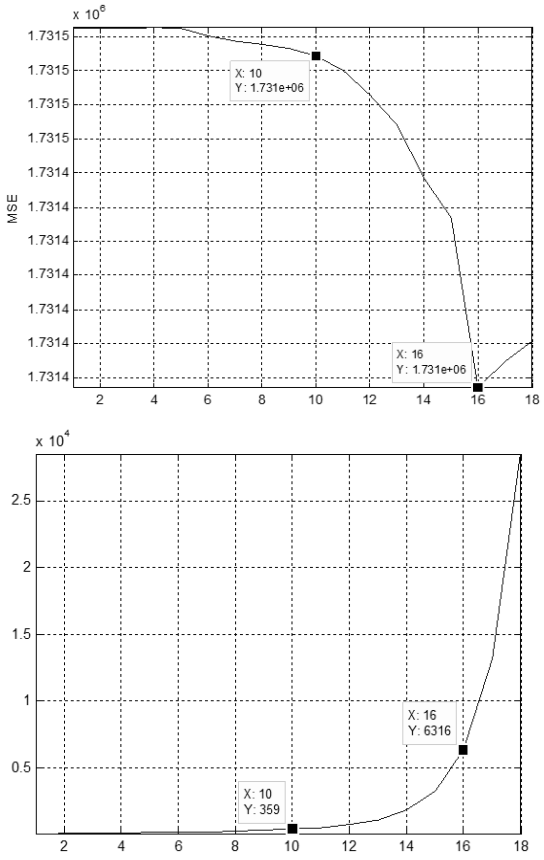


Figure 4. Descomposition level a) MSE between the original signal and the reconstructed signal without the approximation coefficients. (b) Execution time.

To verify if the relevant information was maintained, without the DC component, the MSE criterion was applied between the original signal and the reconstructed signal without the approximation coefficients; a sweep of 1 to 18 levels of decomposition is performed looking for the level that allows to reach the minimum MSE. According to Figure 4, the minimum MSE is reached when performing a decomposition at 16 levels but considering the processing time and that the MSE variations are not very large, it was decided to work with a decomposition at 10 levels since when working with this level reduces the processing time by approximately 20 times with respect to working with 16 levels of decomposition. In Figure 5 can see the result of this procedure on a section of the MFL signals where there is a defect which is highlighted in gray, the result was similar for all other signals.

### *C. Selection of window width and descriptors for the classification stage*

For the design of the classification system we will use descriptors such as the mean, the standard deviation and the interquartile range of the signals in the time domain and the

mean, the standard deviation, the interquartile range, the kurtosis and the asymmetry of the density spectral power [11] [12].

For the calculation of the descriptors, the best window width that maximizes the separability between the two classes is previously identified using the Mann Whitney U test, which is a nonparametric test to verify if the medians of two samples are independent. A rectangular window is defined, in which the width of the window was modified from 16 to 256 samples, making increases in the width in power of 2, that is, 16, 32, 64, 128 and 256 samples, this because the algorithms used work more efficiently. The methodology that was followed in this stage is the following: as the window of width W goes through any signal of the type of approximation Aps (J) and the descriptor X is calculated, two vectors are generated simultaneously corresponding to each class, that is, defect and not defect. To determine if the descriptor X of the window with a W width corresponds to a defect or no defect, the average of the label window is checked. If the value is less than zero, it is said that the data corresponds to the first group, otherwise it is said to correspond to the second group. Once the window finishes crossing each signal, the Mann - Whitney U test is evaluated from the vectors generated, the process is repeated until all the signals of the Aps (J) are made and the average of the p Value corresponding to an X descriptor with a W window width for the type of approach worked. The process is resumed with the following window width W + 1 and once it has been calculated with all the window widths, the entire process is performed again for the following X + 1 descriptor. The process continues until we have determined the average of the p-Value of all the signals, descriptors and window widths of each type of approach. Due to the great length of the signals, we worked with a section of the signal, 600,000 samples, taking the 3 defects of the original signal and 100,000 samples before and after each of them.

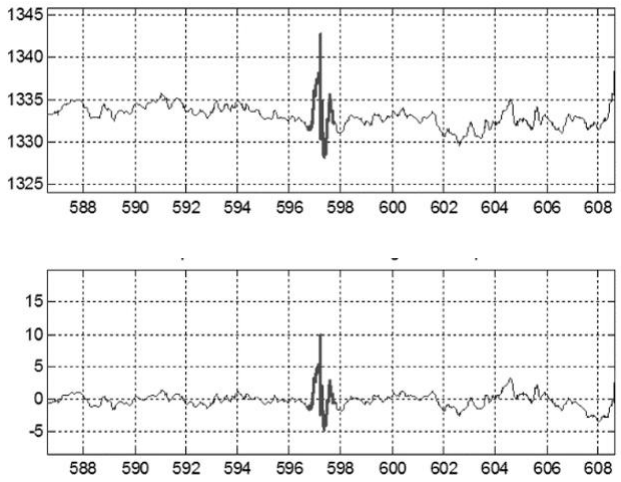


Figure 5. Correction of baseline on the first defect.

The results of the previous analysis for the approximations Aps1 and Aps2 are shown in figures 6 and 7 respectively, some figures are plotted in logarithmic scale to correctly appreciate the results. The abbreviations ST and PSD in the graphs indicate that the signal descriptor was calculated in the time domain or the power spectral density, respectively. The criterion to determine if a descriptor with a certain window width allows a good separability between the classes is to verify if the p-Value is less than 0.05.

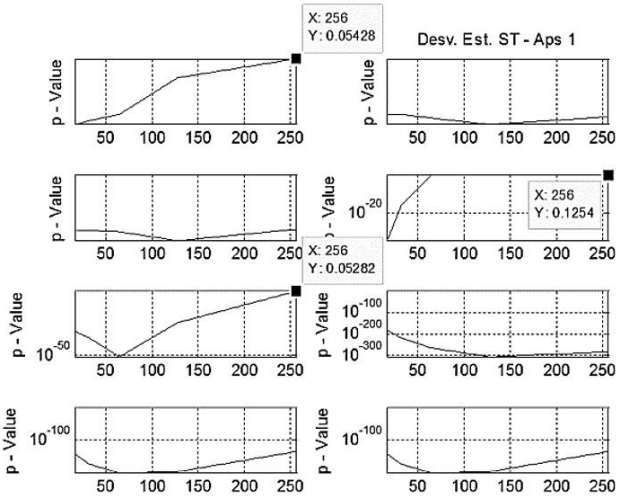


Figure 6. p-Value - Approximation Aps1.

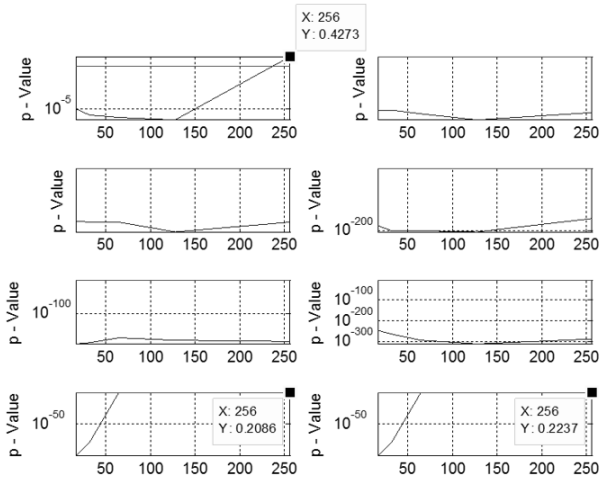


Figure 7. p-Value - Approximation Aps2.

According to the results for the signal type Aps1 all the descriptors work using a window width of 32 samples, this in practice may not be very efficient since a very small window width contains less information. For purposes of reducing the processing time and the number of descriptors, we will work with a window width of 256 samples using only the standard deviation and interquartile range of the signal in time and interquartile range, kurtosis and asymmetry of the power spectral density, since according to the test these descriptors remain below the 0.05 cut. For the signal type Aps2 all the descriptors work with a window width of 128 samples, but applying the same criteria mentioned above, the dimensionality can be reduced using a window width of 256

samples and using the descriptors that are kept below the cut, that is, standard deviation, interquartile range of the signal in time and mean, standard deviation and the interquartile range of the power spectral density.

## III. RESULTS

For the training stage of the classifier, the cross-validation technique was used, which consists of dividing the training patterns in K subsets, r subsets are used as test data and the rest (K-r) as training data. To generate the set of training patterns, the eight signals of a certain type of approach were taken and a vector with all the defect patterns was created, then another vector was created where the same number of non-defect patterns were stored randomly from all the signs. A training pattern corresponds to the 5 calculated descriptors of a window of 256 samples of a signal and the displacement of said window by the signal was made of a 1 sample. To evaluate the performance of the classifier, the confusion matrix was used [12]. In this method, the count of 4 elements is performed: the true positives (TP) are the elements of the class 1 that the classifier frames as class 1, the false negatives (FN) are the elements of class 1 that the classifier marks as class 2, the false positives (FP) are the elements of class 2 that the classifier frames as class 1 and the true negatives (TN) are the elements of case 2 that the classifier marks as class 2. To quantify the performance of the classifier we used the balanced precision index (IPB), this index is basically the classification success percentage, giving equal weight to each of the classes, avoiding a false measurement in highly unbalanced systems. The formula to calculate the balanced precision is equation 3.

$$IPB\ (\%) = \left(\frac{0.5*TP}{TP+FN} + \frac{0.5*FN}{FN+TN}\right) * 100 \quad (3)$$

In addition, the accuracy is verified for each of the classes independently, the expressions to determine the accuracy of class 1 and class 2 are equations 4 and 5.

$$IPB\_clase\ 1\ (\%) = \left(\frac{TP}{TP+FN}\right) * 100 \quad (4)$$

$$IPB\_clase\ 2\ (\%) = \left(\frac{FN}{FN+TN}\right) * 100 \quad (5)$$

Two different classifiers based on artificial neural networks, multilayer perceptron, are proposed for the two approaches. Various learning algorithms existing in the Matlab® 2014a software were analyzed for the classifiers, with the Bayesian regularization method presenting better results. For the classifier that uses the type of approach Aps1, a structure of 5 entries was selected, three hidden layers each with 5, 20 and 10 neurons. Hyperbolic tangent activation functions were used to include the nonlinear dynamics in the network and maintain consistency with the tags. The output layer is a saturated linear function between +1 and -1. For the classifier that uses the type of approach Aps2, a structure of 5 inputs was selected, two hidden layers each with 5 and 25 neurons. The other parameters are equal to the fore mentioned classifier. The results of both classifiers from the training data, after the 50 runs, show a similar performance, as shown in figure 8.

Each classifier was evaluated independently for the eight MFL signals, each with 10,139,190 samples, storing the label signal, result of the classification. The eight signals were compared, term by term, to generate a general label signal. If at the same point the eight signals indicate that there is a defect, that is, they all have a <-1>, a <-1> is assigned at the corresponding point in the general label signal, otherwise if at least one signal indicates that there is no defect, that is, there is one or more <+1>, a <+1> is assigned to the label signal. Finally, to soften the tag signal by eliminating possible small sample errors, a second order low pass filter with 10Hz cutoff frequency was applied to the general label signal and subsequently binarized.

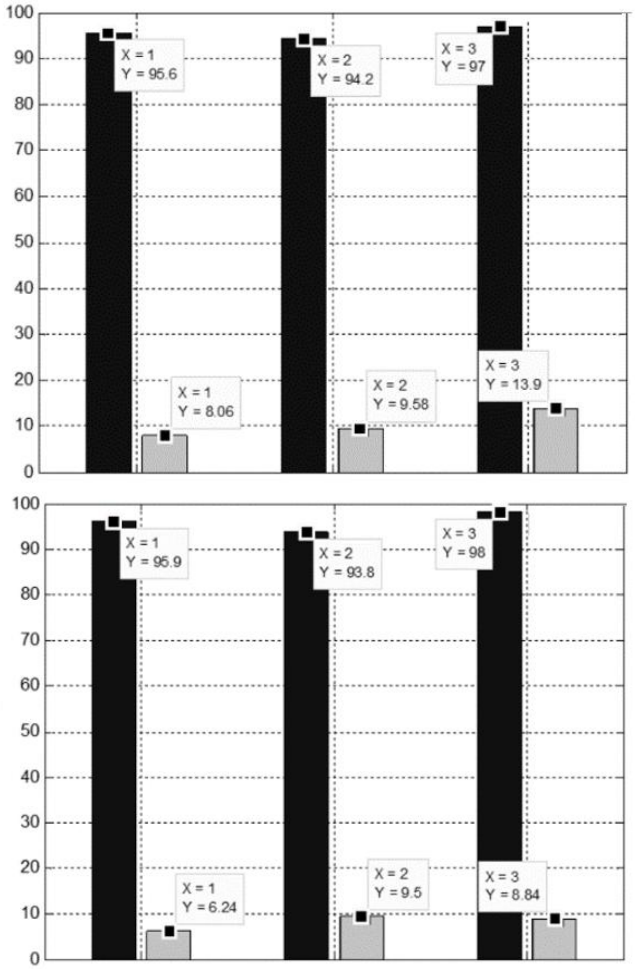


Figure 8. Balanced precision of classifier Aps1 (a) and Aps2 (b).

The general results for both classifiers are shown in Tables 3 and 4, corresponding to the confusion matrices. As can see, the performance of the classifier Aps1 is high since of the 10'138.549 of patterns that were not defective it classified bad 64.204 and of the 641 patterns that are defective it classified badly 23. On the other hand, the performance of the classifier Aps2 is still high but it was

lower than the previous one because of the 10,138,549 of patterns that were not defective, it classified badly, and 8,821 of the 641 patterns that are defect classified as poor 25. Both classifiers based on neural networks have a high performance, but it can be said that the classifier that uses the type of approximation Aps1 is better, since it reduces the number of misclassified patterns by approximately half with respect to the classifier that uses the type of approximation Aps2.

TABLE III. CONFUSION MATRIX FOR CLASSIFIER APS1 WITH COMPLETE SIGNALS

| | **Actual** | |
|---|---|---|
| | + | - |
| **Foretold +** | *10'074.345* | *23* |
| **Foretold -** | *64.204* | *618* |

TABLE IV. CONFUSION MATRIX FOR CLASSIFIER APS1 WITH COMPLETE SIGNALS

| | **Real** | |
|---|---|---|
| | + | - |
| **Foretold +** | *10'002.722* | *25* |
| **Foretold -** | *135.827* | *616* |

## IV. CONCLUSIONS

Because the Shrinkage filter is a non-linear and adaptive filtering technique since it recalculates its parameters (weights and scaling) for each of the windows taken from the signal, it makes it an ideal tool for this application, since the levels of noise can be very variable and depend on several factors. The low number of defect patterns in the database made the process of selecting descriptors and training difficult, for this reason various methodologies were applied where the training stage of the classifier was balanced, taking representative and random samples of the signals and reducing the dimensionality, to achieve the greatest possible generalization and learning of the problem, trying to avoid the memorization of it by the classifiers. The balanced precision allowed to adequately evaluate the performance of the classifiers since having such a high number of patterns of one class compared to such a low number of another is necessary to use an index that equally favors each of them.

## ACKNOWLEDGMENT

This work is carried out thanks to the participation of institutions committed to the generation of knowledge and alternative solutions to problems of the Colombian industry. The company Transportadora de Gas Internacional - TGI, and the Colombian Institute of Science and Technology - COLCIENCIAS are gratefully acknowledged., from the project development of ITION-E inspection tools. In addition, the important cooperation between the Corporations for Corrosion Research (CIC) and the Autonomous University of Bucaramanga (UNAB), especially the GICYM research group, is highlighted.

## REFERENCES

[1] M. Adzal, S. Udpa, "Advanced signal processing of magnetic flux leakage data obtained from seamless steel pipeline". NDT&E International, 35, 449-457, 2002.

[2] J. Tao, Q. Peiwen, Liang, Ch. L. Liang. "Research on a Recognition Algorithm for Offshore-Pipeline Defects during Magnetic-Flux Inspection". Russian Journal of Nondestructive Testing, 41 (4), 231–238, 2005

[3] A. Sadr, S. Ehteram. "Intelligent defect recognition from magnetic flux leakage inspection". NDT.net - The e-Journal of Nondestructive Testing, 2008.

[4] S. Ehteram, S. Moussavi, M. Sadeghi, S. Mahdavi, A. Kazemi. "Intelligent Monitoring Approach for Pipeline Defect Detection from MFL Inspection". Journal of Convergence Information Technology, 5 (2), 2010.

[5] G. Song-wei, M. Feng-ming, Y. Li-jian. "Study on intelligent quantitative recognition of defect in pipeline magnetic flux leakage inspection". Asia-Pacific Conference on NDT. 2006.

[6] W. Lord, D. Oswald, "Leakage field methods of defect detection". International Journal of Nondestructive Testing, 4, 1972.

[7] D. Akilla. "Analysis of magnetic flux leakage signals for surface defects in coiled tubing". M. Sc. Tesis. Tulsa University. 2004

[8] C.A Arizmendi. "Signal processing techniques for brain tumour diagnosis from magnetic resonance spectroscopy data". Tesis de Doctorado, Universidad Politécnica de Cataluña. 2011.

[9] D.R. Llanos Ferraris, V. Cardeñoso Payo. "Filtrado de señales de voz a través de wavelet shrinkage". Publicado en las Actas IV Jornadas de Informática, organizadas por el Grupo de Arquitectura y Concurrencia (GAC), Departamento de Ingeniería Telemática, Universidad de Las Palmas de Gran Canaria. Depósito Legal GC-582-1998, ISBN 84-87526-61-6, 1998.

[10] S. Mukhopadhyay, G.P. Srivastava, "Characterisation of metal loss defects from magnetic flux leakage signals with discrete wavelet transform". NDT&E International, 33, 57-65, 2002.

[11] L. S. Correa, B. F. Giraldo, E. Laciar, A. Torres. "Multi-parameter Analysis of ECG and Respiratory Flow Signals to Identify Success of Patients on Weaning Trials". Annual International Conference of the IEEE EMBS, 32, 6070-6073, 2010

[12] H. Gonzalez, H. Acevedo, C. Arizmendi, B. F. Giraldo, "Methodology for determine the moment of disconnection of patients of the mechanical ventilation using discrete wavelet transform". International Conference on Complex Medical Engineering – ICME. ISBN: 978-1-4673-2971-2 ed: IEEE Publications , p. 483 – 486, 2013.